

# Analysis of new particle formation events and comparisons to simulations of particle number concentrations based on GEOS-Chem/APM in Beijing, China

Kun Wang<sup>1</sup>, Xiaoyan Ma<sup>1\*</sup>, Rong Tian<sup>1</sup>, Fangqun Yu<sup>2</sup>

5 <sup>1</sup>Key Laboratory for Aerosol-Cloud-Precipitation of China Meteorological Administration, Nanjing University of Information Science & Technology, Nanjing 210044, China

<sup>2</sup>Atmospheric Sciences Research Center, University at Albany, Albany, NY, USA.

*Correspondence to:* Xiaoyan Ma (xma@nuist.edu.cn)

**Abstract.** Aerosol particles play important roles in air quality and global climate change. In this study, we analyze the  
10 measurements of particle size distribution from March 12th to April 6th, 2016 in Beijing to characterize new particle formation  
(NPF) by using the observational data of sulfuric acid, meteorological parameters, solar radiation, and fine particles (PM<sub>2.5</sub>,  
particulate matter with diameters less than 2.5  $\mu\text{m}$ ) mass concentration. During this 26-day campaign, 11 new particle formation  
events are identified with obvious bursts of sub-3 nm particle number concentrations and subsequent growth of these nucleated  
particles. It is found that sulfuric acid concentration in Beijing does not have a significant difference between NPF and non-  
15 event days. Low relative humidity (RH) and high daily total solar radiation appear to be favorable to the occurrence of NPF  
events, which is quite obvious in this campaign. The simulations using four nucleation schemes, i.e., H<sub>2</sub>SO<sub>4</sub>-H<sub>2</sub>O binary  
homogeneous nucleation (BHN), H<sub>2</sub>SO<sub>4</sub>-H<sub>2</sub>O-NH<sub>3</sub> ternary homogeneous nucleation (THN), H<sub>2</sub>SO<sub>4</sub>-H<sub>2</sub>O-ion binary ion-  
mediated nucleation (BIMN), and H<sub>2</sub>SO<sub>4</sub>-H<sub>2</sub>O-NH<sub>3</sub>-ion ternary ion-mediated nucleation (TIMN), based on a global chemistry  
transport model (GEOS-Chem) coupled with an advanced particle microphysics (APM) model, are conducted to study the  
20 particle number concentrations and new particle formation process. Our comparisons between measurements and simulations  
indicate that BHN scheme and BIMN scheme significantly underestimate the observed particle number concentrations, and  
the THN scheme captures well the total particle number concentration on most NPF event days but fails to capture the  
noticeable increase in particle number concentrations on March 18th and April 1st. TIMN scheme has obvious improvement  
in terms of total and sub-3 nm particle number concentrations and nucleation rates. This study provides a basis for further

25 understanding of nucleation mechanism in Beijing.

## 1 Introduction

New particle formation (NPF) is the process by which gaseous pollutants transform into particles (gas-particle reaction) then grow into particles with larger particle size through further collision and condensation, which is the main source of particle number abundance generated by secondary transformation in the atmosphere (Yu et al., 2008; Merikanto et al., 2009).

30 With the development of industry and the increase of human activities, air quality is deteriorating day by day, and atmospheric particulate matter has become one of major sources of air pollutants. Particulate matter not only affects the radiation balance by scattering and absorbing solar radiation, but also indirectly modifies the climate by acting as cloud condensation nuclei (CCN) (Merikanto et al., 2009). In addition, new particles can also impact the formation of fog and haze. NPF is capable of increasing PM<sub>2.5</sub> mass concentration and haze particle (diameter > 100 nm) number concentration (Kulmala  
35 et al., 2022). In the context of the decline in pollutant emissions caused by the lockdown during the COVID-19 epidemic, new particles derived from NPF played a significant role in the formation of haze (Tang et al., 2021). Guo et al. (2014) found that after an NPF event, smog-haze pollution continued to occur in Beijing, indicating that aerosol nucleation and growth led to the development of PM<sub>2.5</sub>. When the concentration of atmospheric particulate matter is high, atmospheric visibility will be reduced in fog and haze weather, and high concentration of atmospheric fine particulate matter will also harm human health (Kaiser,  
40 2005) as tiny aerosol particles can enter the human body through the respiratory system.

At present, the nucleation and growth of new particles has been widely studied around the world. Sipilä et al. (2010) demonstrated a positive relationship between nucleation rate and sulfuric acid concentration. Kulmala et al. (2013) established a framework of atmospheric nucleation at three different scales below 2 nm based on observations, identifying the participation of sulfuric acid in the nucleation process and emphasizing the important role of organic compounds in atmospheric aerosols.  
45 A positive correlation between nucleation rate and sulfuric acid concentration (or H<sub>2</sub>SO<sub>4</sub> proxy) was also found in many NPF studies in China (Xiao et al., 2015; Dai et al., 2017).

Besides sulfuric acid, a number of other nucleating precursors, including atmospheric ions, amines, ammonia, iodine oxides, and organic acids, have been proposed to be involved in the formation of the critical nucleus under different ambient

environments. Amines and ammonia are crucial in NPF because of their ability to stabilize sulfuric acid clusters by forming  
50 acid-base complexes (Yao et al., 2018). Currently several major theories have been proposed to explain the phenomenon of  
nucleation in the atmosphere, including the classical binary nucleation theory (Hussein, 2005) such as H<sub>2</sub>SO<sub>4</sub>-H<sub>2</sub>O binary  
nucleation (Kulmala et al., 1998), H<sub>2</sub>SO<sub>4</sub>-NH<sub>3</sub>-H<sub>2</sub>O ternary nucleation (Korhonen et al., 1999), ion-mediated nucleation (Yu  
and Turco, 2000), organic compounds participated nucleation (Wang et al., 2015). HIO<sub>3</sub> nucleation mechanism is found to  
dominate NPF in the coastal regions (Sipilä et al, 2016).

55 There are some special features associated with NPF events found in China. For example, the concentrations of nucleating  
precursors and pre-existing aerosol particles both can be quite high in polluted cities, which is different from cleaner  
environments (Kulmala et al., 2016). The observed nucleation rate of 1.5 nm particles and NPF frequency in urban Beijing  
usually show an obvious seasonal variation with maxima in winter (Deng et al., 2020). Jayaratne et al. (2017) conducted the  
observations in Beijing during the winter of 2015 and did not observe any NPF event when the daily mean PM<sub>2.5</sub> concentrations  
60 were higher than 43 µg/m<sup>3</sup>. However, in some cases, the condensation sinks (CS) or the average coagulation sinks are not  
significantly lower during NPF events compare to non-NPF times, suggesting that other factors, such as the precursor vapor  
and photochemical activity, may also play an important role in driving NPF (Gong et al., 2010). Yan et al. (2021) found that  
sulfuric acid and base molecules were responsible for the initial steps of NPF during a wintertime measurement in Beijing. In  
addition, H<sub>2</sub>SO<sub>4</sub>-amine nucleation can explain the observed high new particle nucleation rate under the high coagulation sink  
65 and dimethylamine (DMA) is the key base for H<sub>2</sub>SO<sub>4</sub>-base nucleation in highly polluted urban environments (Cai et al., 2021,  
2022). Beijing is a representative city in northern China because of its developed industry and commerce, and thus quite high  
concentrations of atmospheric precursors and pre-existing aerosol particles. Wu et al. (2007) found that NPF days accounted  
for 40% of the observation days from March 2004 to February 2005 in Beijing, which are usually sunny and dry days.  
Continuous and comprehensive long-term observations will help to understand the mechanism of NPF, and answer the key  
70 participants and processes of NPF under complex air conditions in China. Besides, laboratory experiments and model  
simulations will also be very necessary. Chen et al. (2019) investigated the effect of organics involved nucleation scheme on  
NPF in Beijing, but previous model studies and comparisons based on different nucleation schemes in Beijing are still lacking.

Since nucleation is a key process controlling particle properties in the atmosphere. To better understand the formation

and evolution mechanisms of air pollution, especially in heavy pollution areas, it is necessary to assess the applicability of  
75 nucleation parametrizations currently available. This study aims to evaluate the performance of four currently widely-used  
nucleation schemes, and provide some clues on the contribution of different nucleation pathways to aerosol number  
concentrations. The paper is organized as below. We first analyze the favorable background of new particle formation in Beijing,  
and then conduct the simulations using four nucleation schemes, i.e.,  $\text{H}_2\text{SO}_4\text{-H}_2\text{O}$  binary homogeneous nucleation (BHN) (Yu,  
2007, 2008),  $\text{H}_2\text{SO}_4\text{-H}_2\text{O-NH}_3$  ternary homogeneous nucleation (THN) (Yu, 2006a),  $\text{H}_2\text{SO}_4\text{-H}_2\text{O-ion}$  binary ion-mediated  
80 nucleation (BIMN) (Yu, 2006b), and  $\text{H}_2\text{SO}_4\text{-H}_2\text{O-NH}_3\text{-ion}$  ternary ion-mediated nucleation (TIMN) (Yu et al., 2018), based  
on a global chemistry transport model (GEOS-Chem), and compare with the observed NPF events from the measurements  
from March 12th to April 6th, 2016 in Beijing to understand the nucleation mechanism.

## 2 Methodology

### 2.1 Observations

85 The observational data used in this paper include particle size distributions, temperature (T), relative humidity (RH), and  
sulfuric acid concentration, which was provided by Cai et al. (2017a). The measurement field was located on the top floor of  
a four-story building in the center of the campus of Tsinghua University in Beijing, and all observations were collected during  
the period from March 12th, 2016 to April 6th, 2016. A home-made diethylene glycol scanning mobility particle spectrometers  
(DEG-SMPS) was used to measure 1-5 nm particle size distributions and the particle size distributions from 3 nm to 10  $\mu\text{m}$   
90 (in aerodynamic diameter, Liu et al., 2016) were measured by a particle size distribution system (including a TSI aerodynamic  
particle sizer and two parallel SMPSs, equipped with a TSI nano-DMA and a TSI long DMA, respectively) with a resolution  
of 5 minutes. A specially designed miniature cylindrical differential mobility analyzer (mini-cyDMA) for effective  
classification of 1-3 nm (sub-3 nm) aerosol was equipped with the DEG-SMPS (Cai et al., 2017b). Sulfuric acid was measured  
by a modified high-resolution time-of-flight chemical ionization mass spectrometer (HR-ToF-CIMS, Aerodyne Research Inc.)  
95 with a resolution of 5 minutes. Further details of the measurement methods can be found in Cai et al. (2017a).

In addition, the daily  $\text{PM}_{2.5}$  mass concentration provided by the China National Environmental Monitoring Center

(<http://www.cnemc.cn/>, last access: 20 November 2022), and solar radiation datasets, including daily maximum solar radiation flux density and the daily total solar radiation, measured from the National Meteorological Information Center of the China Meteorological Administration (<http://data.cma.cn/>, last access: 20 November 2022), are also employed in this study.

## 100 2.2 Model description

The GEOS-Chem model is a global three-dimensional chemical transport model driven by assimilated meteorological observations from the Goddard Earth Observing System (GEOS) of the NASA Global Modeling Assimilation Office (GMAO). The GEOS-Chem model includes a detailed simulation of tropospheric O<sub>3</sub>-NO<sub>x</sub>-hydrocarbon chemistry as well as aerosols and their precursors (Park et al., 2004). An advanced particle microphysics (APM) model has been coupled with GEOS-Chem to  
105 study detailed particle formation and growth processes in the global atmosphere (Yu and Luo, 2009). The APM model is an advanced multi-type, multi-component, size-resolved microphysics code developed for explaining atmospheric particle observations (e.g., Yu, 2006b; Yu and Luo, 2009; Yu and Turco, 2011). The basic microphysical processes in APM include nucleation, coagulation, condensation/evaporation, thermodynamic equilibrium with local humidity, and dry deposition. In  
110 GEOS-Chem/APM, sulfate (or secondary) particles are represented by 40 sectional bins with dry diameters ranging from 1.2 nm to 12 μm, including 30 bins for 1.2–120 nm and another 10 bins for 0.12–12 μm. In the model, new particle formation is parameterized by ion-mediated nucleation (IMN) which is based on physics and constrained by laboratory data (Yu, 2006b) and can finely predict global nucleation distributions with a reasonable consistency (Yu et al., 2008). In addition, the IMN takes into account the complex interactions among small air ions, neutral and charged clusters of various sizes, precursor vapor molecules, and pre-existing aerosols. The growth of nucleated particles through the condensation of sulfuric acid vapor and  
115 equilibrium uptake of nitrate, ammonium, and secondary organic aerosol (SOA) is explicitly simulated, along with the scavenging of secondary particles by primary particles (dust, black carbon, organic carbon, and sea salt) (Yu and Luo, 2009). Yu (2011) has further developed the APM module to explicitly calculate the co-condensation of H<sub>2</sub>SO<sub>4</sub> and low-volatility secondary organic gases (LV-SOGs) or low-volatility organic compounds (LVOCs) on secondary particles and primary particles. The aerosol simulation considered the successive oxidation aging of the oxidation products of various volatile organic  
120 compounds (VOCs) (Yu, 2011). New particle formation and particle number concentrations predicted by the GEOS-

Chem/APM model have been extensively evaluated against a wide range of aircraft-, land-, and ship- based field data (Yu and Luo, 2009, 2010; Yu et al., 2010). In recent years, the APM model has also been coupled with other numerical models such as Nested Air Quality Prediction Modeling System (NAQPMS) and Weather Research and Forecast/Chemistry (WRF-Chem) model to study new particle formation (Luo and Yu, 2011; Chen et al., 2019).

125 In this study, we use a version of GEOS-Chem (v12.6.0) driven by the GEOS-FP-assimilated meteorological field, with a spatial resolution of  $2^\circ \times 2.5^\circ$  and 47 vertical levels during the period of March 1st, 2016 to April 7th, 2016. We focus on four nucleation schemes to compare simulations with particle number concentration measurements from March 12th to April 7th in this study.

### 3 Results and discussions

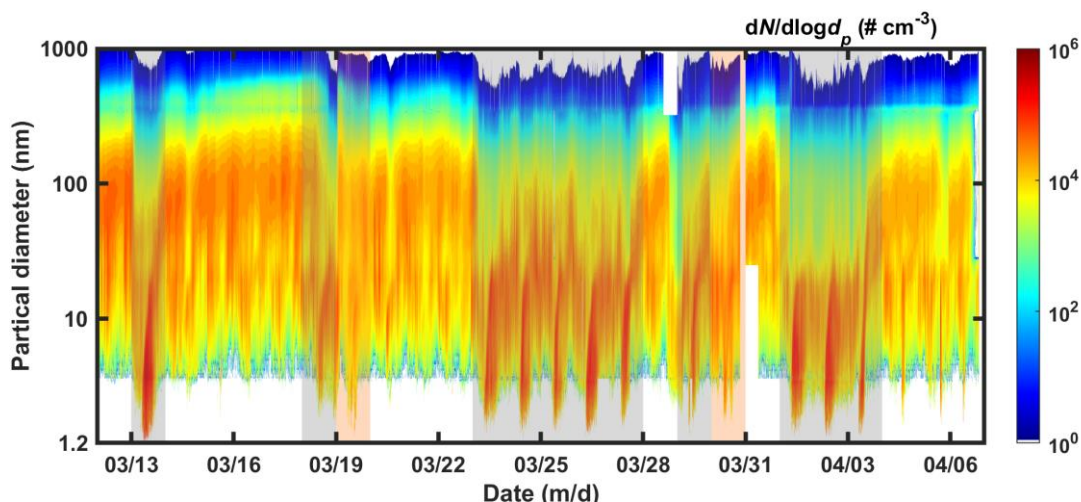
#### 130 3.1 Occurrence of new particle formation events

NPF generally includes the following two steps: (1) condensable vapors are produced via chemical reactions then gaseous vapors form critical clusters through gas-particle reaction, (2) the critical clusters continue to grow to a larger size (1-2 nm) (Kulmala et al., 2013) and compete with pre-existing particles to survive in the collision and removal processes at the same time, in this quasi-steady-state process, new particles can only be formed when growth is dominant.

135 Currently, there is no unique mathematical criterion or definition for NPF events. Dal Maso et al. (2005) proposed a criterion to justify NPF events, i.e., a new mode of particles start in the nucleation-mode size range, and prevail within a few hours and show signs of growth. The days without the particles in the nucleation-mode are called non-event days. It is noted that some days are not easily classified as either NPF days or non-event days, so these days are usually classified undefined days. The criteria to determine NPF in this study are as follows: (1) high concentrations of sub-3 nm clusters/particles appear  
140 over a time of hours at the onset of the event, (2) subsequent growth to larger sizes for a few hours.

Figure 1 shows the particle size distributions observed during March 12th, 2016-April 6th, 2016 in Beijing. According to the criteria of NPF events defined above, 11 typical event days and 13 non-event days are identified during the 26-day campaign. The other 2 days, i.e., March 19th and 30th, the sub-3 nm particle number concentration is relatively low and the evolution of

particle size distributions is not continuous, are identified as undefined days. The NPF events are observed with a high  
145 frequency (42%) in spring in this campaign, which is similar to the previous study in Beijing (Wu et al., 2007) in which they  
found that spring is usually the season with the highest frequency of NPF events in northern China. One explanation is that  
stronger wind from the north removes pre-existing particles to create a clean regime, which further leads to the occurrence of  
NPF events (Wu et al., 2008; Cai et al., 2017a; Chu et al., 2019; Wu et al., 2020).



150 **Figure 1. Contour of measured particle size distributions from March 12 to April 6, 2016. The identified 11 NPF days and 2 undefined days are shadowed by grey and orange background, respectively.**

### 3.2 Analysis based on observations

#### 3.2.1 The sulfuric acid concentration on NPF days and non-event days

Since the number concentration of new particulate matter in the atmosphere is strongly dependent on the concentration  
155 of sulfuric acid, so sulfuric acid is a key precursor species for atmospheric nucleation and has an important contribution to  
NPF events (Sipilä et al., 2010). However, it was not easy to measure the concentration of sulfuric acid a few years ago. With  
the development of technology, chemical ionization mass spectrometry (CIMS) was used to detect gaseous sulfuric acid in the  
atmosphere (Zheng et al, 2011, 2015).

The gaseous sulfuric acid in the atmosphere is mainly produced by the oxidation reaction of sulfur dioxide and OH.  
160 Stockwell and Calvert (1983) demonstrated the reaction as follows:

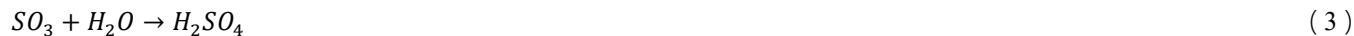
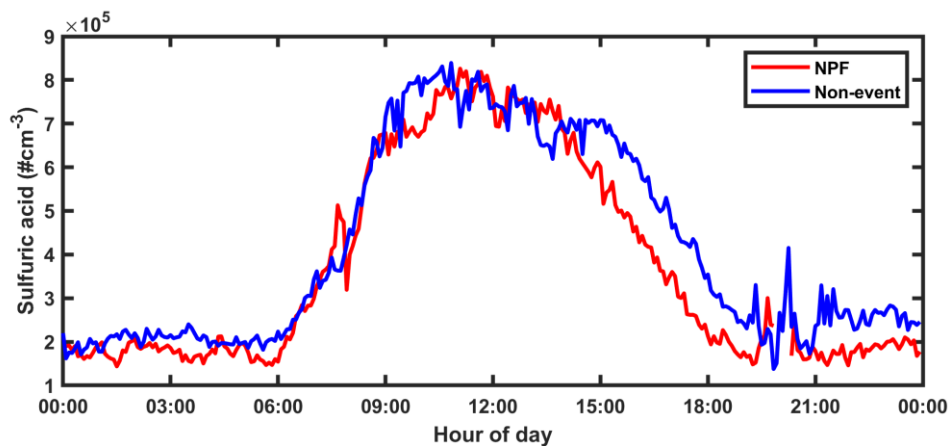


Figure 2 shows the average diurnal concentration of sulfuric acid on the NPF event days and non-event days. The gaseous  $H_2SO_4$  concentrations exhibit significant diurnal variation, and sulfuric acid concentration closely follows the diurnal solar cycle because of its short atmospheric lifetime (less than 1 min) (Zheng et al., 2011). It is known that NPF events usually occur within a few hours after sunrise and end in the afternoon. During the start period, the averaged sulfuric acid concentration on NPF days is close to that on non-event days, and compared to NPF days, the averaged sulfuric acid concentration on non-event days is not significantly low during the whole time period. The average sulfuric acid concentration during non-event periods (605066 ± 312981 cm<sup>-3</sup>) is obviously higher than that between 6:00 and 18:00 on NPF days (560802 ± 251528 cm<sup>-3</sup>).



**Figure 2. Averaged diurnal cycles of sulfuric acid concentrations for NPF days and non-event days during the 26-day measurement period.**

The daily maximum sulfuric acid concentrations measured in this study (> 10<sup>6</sup> cm<sup>-3</sup>) are lower than those in summer of 2017 in Beijing (> 10<sup>7</sup> cm<sup>-3</sup>) (Wu et al., 2020) and close to those in winter of 2019 in Beijing (> 10<sup>6</sup> cm<sup>-3</sup>) (Foreback et al., 2022). This might be caused by the relatively weak solar radiation intensity in springtime and wintertime measurements compared with summertime observation. In this study,  $H_2SO_4$  in Beijing during the campaign period is sufficiently high for nucleation to occur and NPF events appear to be governed by aerosol Fuchs surface area (which is a representative parameter



of coagulation scavenging) (Cai et al., 2017a). Yan et al. (2021) also found that observed H<sub>2</sub>SO<sub>4</sub> concentrations were higher  
180 on non-NPF days than on NPF days in the winter of 2018. Therefore, it is shown that the sulfuric acid concentration in Beijing  
is sufficient to lead to NPF, which is consistent with some earlier studies in Nanjing (An et al., 2015; Qi et al., 2015) and  
Shanghai (Xiao et al., 2015). There is usually enough SO<sub>2</sub> for NPF to occur under heavily polluted conditions (Herrmann et  
al., 2014). The observed SO<sub>2</sub> concentrations during October 2015 showed that the most polluted area was located in Northern  
China (Hu et al., 2022). The surfaces of atmospheric aerosols correspond to the major sink for gas-phase sulfuric acid, but an  
185 increase in atmospheric sulfuric acid does not always result in more frequent NPF events (Zhang et al., 2012). So far, the  
presence of gaseous sulfuric acid in concentrations exceeding 10<sup>5</sup> molecules cm<sup>-3</sup> has been shown as a necessary condition to  
occur NPF in the atmosphere (Weber et al., 1999; Nieminen et al., 2009). Overall, the previous results seem to indicate that  
adequate sulfuric acid concentration was not a limiting factor for NPF in Chinese megacities even if it was necessary.

### 3.2.2 Solar radiation and meteorological conditions for NPF

190 Air pollutants and meteorological conditions are usually studied together with nanoparticles and their precursors. By  
comparing the pollution characteristics between NPF event and other non-event days, we can obtain some clues on key factors  
affecting NPF events. Figure 3 shows the scatter plots of the daily total solar radiation and relative humidity color coded with  
PM<sub>2.5</sub> mass concentration. The daily values were averaged between 8:00 and 16:00 because NPF events usually occur during  
the daytime. It is found that the favorable conditions on NPF days were similar, which were significantly different from the  
195 conditions on non-event days.

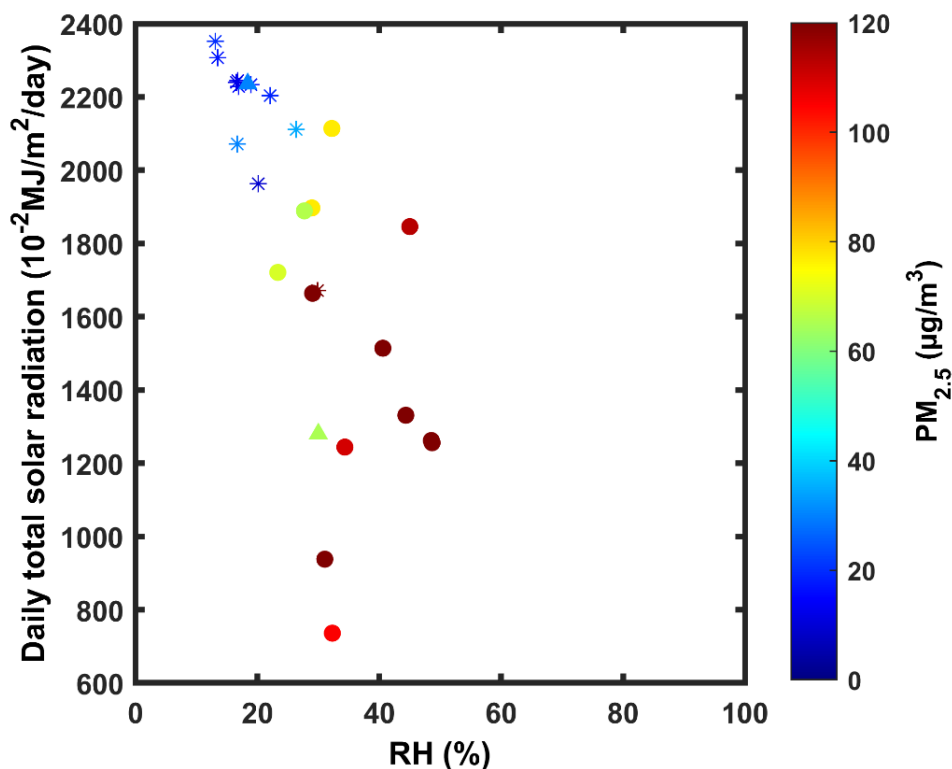


**Figure 3. Scatter plot of NPF days (asterisks), non-event days (circles), and undefined days (triangles) between daily total radiation and RH color coded with PM<sub>2.5</sub> mass concentration.**

The statistics indicate that the average RH for the 11 NPF days and 13 non-event days was 16% and 37%, respectively, implying that NPF events in Beijing likely occur on days with low relative humidity. The explanation is possibly because that at high RH, coagulation scavenging of sub-3 nm clusters was enhanced, while reduced solar radiation led to gas phase oxidation chemistry was diminished, and also condensation sink of condensable gases was increased due to hygroscopic growth of the pre-existing particles (Hamed et al., 2011). Meanwhile, the variation of solar radiation could influence new particle formation via photochemical process (Shen et al., 2021). Strong solar radiation favors the OH formation by photochemical reaction, then OH involves in processes of sulfate formation and VOCs oxidation, and produces sulfuric acid and vapors with low volatility in the atmosphere. Finally, these vapors with low volatility and sulfuric acid molecules can condense together to form new clusters and lead to NPF (Zhang et al., 2012). Laboratory studies and field observations have indicated that organic vapors participate in the particle nucleation besides sulfuric acid (Metzger et al., 2010; Yao et al., 2018). Qiao et al. (2021) found that

oxygenated organic molecules significantly promoted the growth of 3–25 nm particles. Kulmala et al. (2022) found that the  
210 variability of growth rates of particles originating from NPF depend only weakly on H<sub>2</sub>SO<sub>4</sub> concentrations. In addition, low  
volatility organic compounds were proposed to contribute to the particle growth rate (Tröstl et al., 2016). Sulfuric acid was  
enough to explain the observed growth for particles smaller than 3 nm but was insufficient to explain the observed growth  
rates of large particles (Xiao et al., 2015; Yao et al., 2018). Therefore, when solar radiation was high, the low volatility organic  
vapors generated by VOCs oxidation may promote the particle growth. Besides, it is proposed that solar radiation may create  
215 a turbulence flow and then strengthen the source during nucleation process and reduce the sink in the growth process (Wu et  
al., 2020).

Since the meteorological factors have systematical influences on NPF, it is difficult to isolate the effect of single factor  
on NPF. For example, higher solar radiation intensity usually increases the temperature, but the role of temperature on NPF  
was inconsistent in many studies. Qi et al. (2015) found that NPF was accompanied by a higher temperature in spring, summer  
220 and autumn of 2011-2013 in Nanjing, but Sun et al. (2021) found that temperature had no significant role in NPF in the  
summertime and wintertime in the coastal area of Qingdao, China. Yan et al. (2021) found that mean temperature in NPF and  
non-event days was almost identical during the winter of 2018 in Beijing. It seems that the temperature associated with NPF  
events in various cities/regions have different characteristics. Besides, Xiao et al. (2021) demonstrated that NPF in polluted  
urban environments was largely driven by H<sub>2</sub>SO<sub>4</sub>-base clusters, stabilized by the presence of amines, high ammonia  
225 concentrations and lower temperatures. A negative correlation between PM<sub>2.5</sub> mass concentration and the occurrence of NPF  
events shown in Figure 3 indicates that NPF likely occurs when PM<sub>2.5</sub> concentration and gas pollutant concentrations are both  
low (Wu et al., 2007). Previous study found that high PM<sub>2.5</sub> concentrations suppress NPF by increasing the sinks of vapor  
responsible for nucleation and growth of clusters and nucleation mode particles (Zhou et al., 2020), new particle formation  
will be typically suppressed when the aerosol surface area exceeds 100 μm<sup>2</sup>/cm<sup>3</sup> (Aalto et al., 2001). Wu et al. (2020) found  
230 that unstable atmospheric turbulence will effectively reduce CS by diluting pre-existing aerosol particles and so as to promote  
nucleation. Therefore, more measurements of meteorological parameters and gaseous precursors can help improve our  
understanding on NPF in the future.

### 3.3 GEOS-Chem/APM model simulation

In order to understand the particle nucleation mechanism in polluted areas such as Beijing, and reduce uncertainties in  
235 model simulations and predictions, we conduct the simulations from four nucleation schemes based on GEOS-Chem/APM.  
To ensure the input meteorological parameters are reasonably good and thus reduce the impact on the simulated nucleation,  
we firstly compare the temperature (at 10 m above the displacement height) and RH (at the first layer, about 70 meters above  
the surface) of GEOS-FP input to GEOS-Chem/APM with measurements taken near surface (Figure 4). It is shown that the  
temporal variations of the temperature and humidity input to the model are quite consistent with those of the observations,  
240 though the magnitude of the temperature input to the model is slightly lower than the observed value.

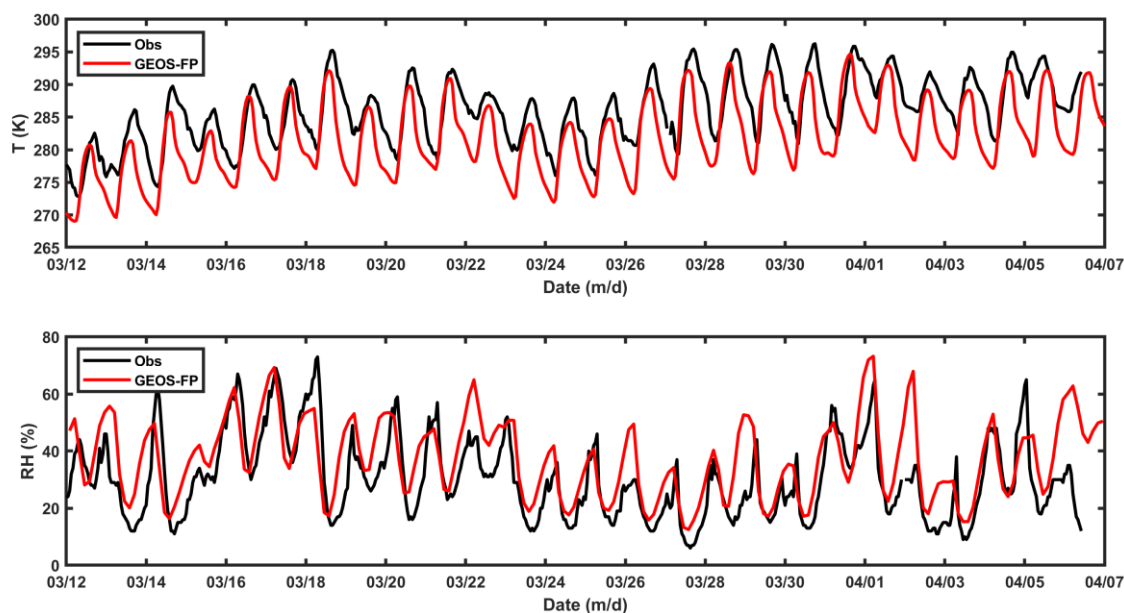


**Figure 4.** Time series of temperature (at 10 m above the displacement height) and RH (at the first layer, about 70 meters above the surface) input to the model and time series of measurements at a height of about 10 meters during the 26-day campaign.

Figures 5 and 6 present the total and sub-3 nm particle number concentrations from the GEOS-Chem/APM simulations  
245 of four nucleation schemes, as well as the observed particle number concentrations, respectively. We found that the simulations  
with BHN and BIMN schemes significantly underestimate the observed total particle number concentrations, and thus cannot

show significant number concentration fluctuation to distinguish NPF event and non-event event days. The simulation with the THN scheme shows the total number concentration fluctuation on most NPF event days but fails to capture the noticeably increase of particle number concentrations on March 18th and April 1st. The simulation with the TIMN scheme reproduces quite well the increase of particle number concentration on all NPF event days, including continuous NPF events on March 23rd to 27th and every discontinuous single NPF event day, but underestimates the observed daily maximum particle number concentration on March 26th, 27th and April 1st.

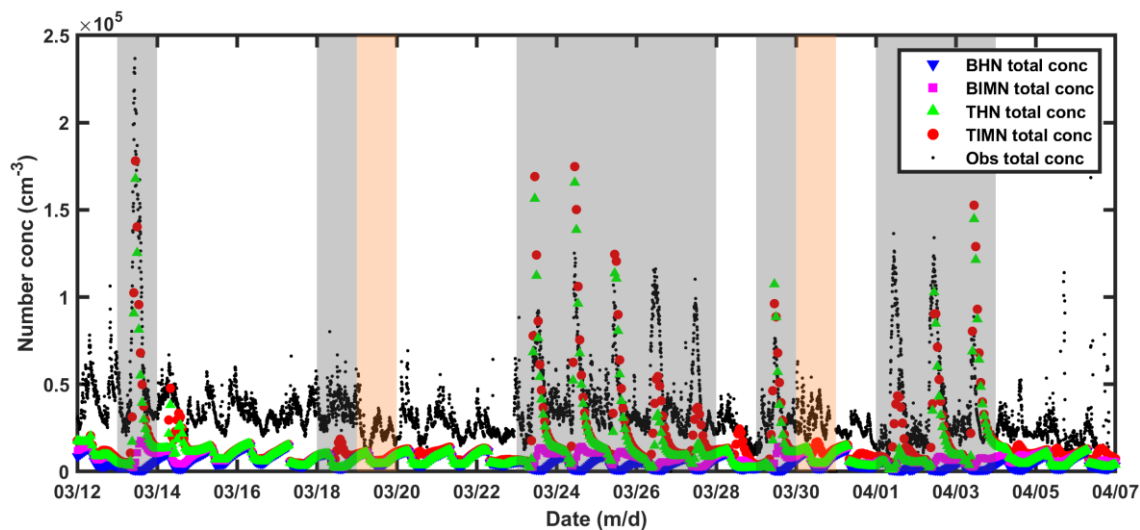


Figure 5. Comparison of observed total particle number concentrations with those simulated on the basis of BHN, BIMN, THN, and TIMN schemes during the measurement period. The identified NPF days and undefined days are shadowed by grey and orange background, respectively.

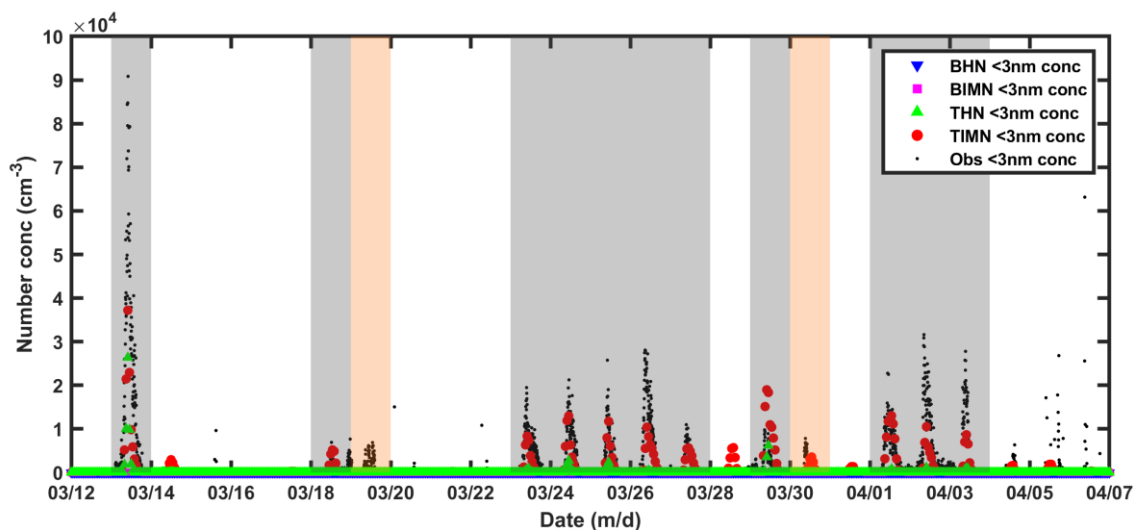


Figure 6. Comparison of observed sub-3 nm particle number concentrations with those simulated on the basis of BHN, BIMN, THN, and TIMN schemes during the measurement period. The identified NPF days and undefined days are shadowed by grey and orange background, respectively.

260

The sub-3 nm particle number concentrations (Figure 6) and nucleation rates (Figure 7) from the simulations with BHN and BIMN are quite close to zero and not sensitive to daily variations. Such low nucleation rates lead to low particle number concentrations in the consequent growth process. The nucleation rates of different schemes in this study were calculated using lookup tables, which captured well the absolute values of nucleation rates and their dependence on key controlling parameters as observed during the well-controlled Cosmics Leaving Outdoor Droplets (CLOUD) experiments (Yu et al., 2020). Some uncertainties may exist in nucleation schemes as a result of uncertainties in the thermodynamics data used in the nucleation model. There are six parameters controlling nucleation rates for TIMN ( $J_{\text{TIMN}}$ ), including sulfuric acid vapor concentration ( $[\text{H}_2\text{SO}_4]$ ), ammonia gas concentration ( $[\text{NH}_3]$ ), temperature ( $T$ ), relative humidity ( $\text{RH}$ ), ionization rate ( $Q$ ), and surface area of pre-existing particles ( $S$ ). Therefore, on the ground, the ion nucleation rates could be limited by ion production rates and cannot produce nucleation rates higher than  $Q$ . Depending on the definition, THN may be treated as a part of TIMN in the ternary nucleation system (Yu et al., 2020). Compared to  $J_{\text{TIMN}}$ , there is one fewer controlling parameter for nucleation rates for THN ( $J_{\text{THN}}$ ) (no  $Q$  dependence) and BIMN ( $J_{\text{BIMN}}$ ) (no  $[\text{NH}_3]$  dependence), while nucleation rate for BHN ( $J_{\text{BHN}}$ ) only depends on four parameters ( $[\text{H}_2\text{SO}_4]$ ,  $T$ ,  $\text{RH}$ , and  $S$ ). The uncertainties in the values of these parameters simulated by the model, as a result of uncertainties in the emissions, chemistry, and meteorology, will affect the simulation results. In addition,

270

275 the real nucleation mechanisms in the atmosphere are complex and may involve additional parameters. Besides, the comparison  
between simulation results based on large grids and measurements also created uncertainties. Yu et al. (2020) found that  
nucleation rates with TIMN agreed with the CLOUD measurements within the uncertainties under nearly all conditions.  
Besides, the comparisons of horizontal spatial distributions of annual mean nucleation rates in the lower boundary layer (0-  
0.4km) simulated with six different nucleation schemes indicated that annual mean nucleation rate based on the BHN scheme  
280 significantly underestimated particle number concentrations (Yu et al., 2010). In contrast, the nucleation rates based on the  
TIMN scheme were high not only on NPF days, but also on some non-event days. Not all these days with high nucleation rates  
have high particle number concentrations as well. Even so, the eventual simulated particle number concentrations show good  
agreement with observations. Nevertheless, the simulated nucleation rates in Figure 7 were lower than the measured particle  
nucleation rates of 1.5 nm particles (Max  $J_{1.5}$ ) reported in Cai et al. (2017a). Besides, nucleation rates measured in urban areas  
285 can be higher than  $10 \text{ cm}^{-3} \text{ s}^{-1}$  (Yao et al., 2018; Yan et al., 2021). The relatively coarse spatial resolution in a global model  
implies that the model produces a regional mean nucleation rate compared to observation. Thus, it is difficult to perfectly  
reproduce the nucleation rate characteristics over urban areas. Nevertheless, we acknowledge that it is possible other nucleation  
mechanisms such as  $\text{H}_2\text{SO}_4$ -amine and  $\text{H}_2\text{SO}_4$ -organics nucleations may also simultaneously contribute to nucleation in  
polluted urban areas, which needs further study in the future.

290 Recent measurements in urban Shanghai found that DMA is perhaps the dominating base to stabilize  $\text{H}_2\text{SO}_4$  clusters (Yao  
et al., 2018). It is good to address the roles of amines in the simulation. However, there is probably a long way to go before  
using the model to address the role of amines in nucleation for the following reasons. Firstly, the parameterization of sulfuric  
acid-amine nucleation scheme is not yet mature enough and a lot of validations against observations need to be done. Secondly,  
there is quite limited information on amine sources and thus all current emission inventories, to our knowledge, do not contain  
295 the inventories for amines. Therefore, it is not possible currently to carry out such simulations.

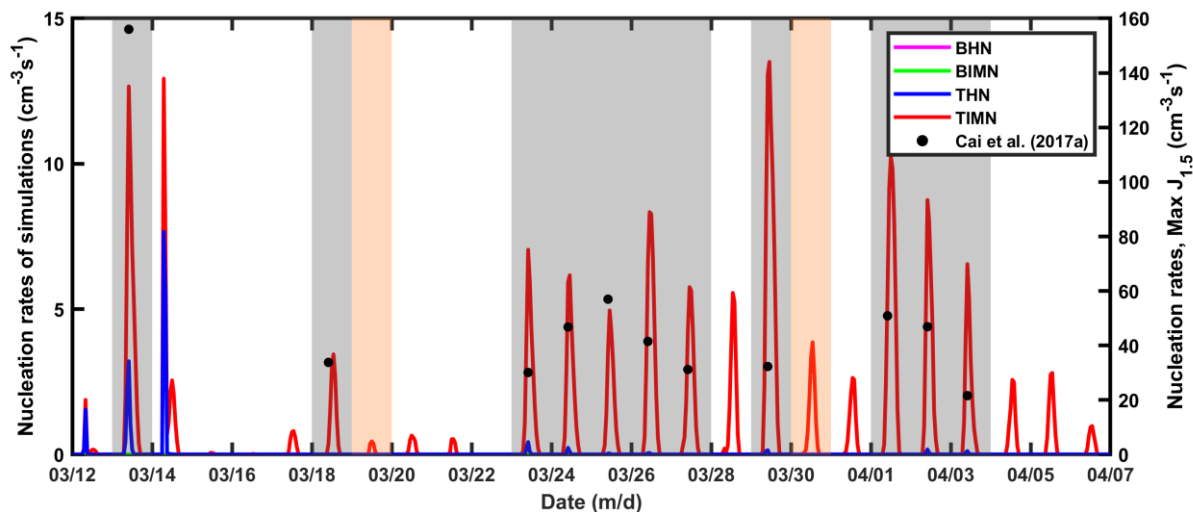


**Figure 7.** Time series of nucleation rates simulated on the basis of BHN, BIMN, THN, and TIMN schemes during the measurement period and the measured particle nucleation rates of 1.5 nm particles ( $\text{Max } J_{1.5}$ ) reported in Cai et al. (2017a). The identified NPF days and undefined days are shadowed by grey and orange background, respectively.

300 Table 1 shows the correlation coefficients between the simulated particle number concentrations and the observed ones during the entire study period and NPF event days. The simulation with BHN and the observation is negatively correlated, indicating that there are obvious differences between the simulated results of BHN and the observed total particle number concentrations. According to the correlation coefficients, the BIMN scheme also performs not well. In contrast, the particle number concentrations with THN and TIMN are positively correlated with the observations, and the correlation coefficients

305 between observations and simulations with TIMN scheme are higher than those with THN, indicating that TIMN has a better performance to simulate NPF events. The correlation coefficients between sub-3 nm particle number concentrations and simulation results based on TIMN scheme (about 0.79) during two periods are significantly higher than those between the total particle number concentrations and simulations (about 0.65).



310 **Table 1. Correlation coefficient of observation total and sub-3nm particle number concentrations with BHN, BIMN, THN and TIMN scheme, respectively.**

	Obs_3nm		Obs_total	
	R <sup>a</sup>	R <sup>b</sup>	R <sup>a</sup>	R <sup>b</sup>
BHN	-0.016	0.006	-0.202**	-0.357**
BIMN	0.134**	0.099	0.016	-0.006
THN	0.773**	0.782**	0.594**	0.586**
TIMN	0.795**	0.793**	0.649**	0.657**

<sup>a</sup> During the measurement period; <sup>b</sup> during NPF days; \*\* the correlation coefficient passes the statistical significant test ( $p < 0.01$ ).

Figure 8 shows the temporal evolution of simulated particle number size distribution based on the TIMN scheme during 26 days in Beijing. According to the same criterion, all NPF days can be identified, which is consistent with observations. On most NPF days, the simulated number concentrations and particle number size distributions are close to observations. However, 315 the simulated particle number size distributions on non-event days are obviously different from Figure 1, because the background number concentration is difficult to simulate. Thus, the simulated number concentrations on most non-event days in Figure 5 are indeed significantly lower than observations. One NPF event on March 28th predicted by the model is not observed with measurements, and the simulated particle number concentrations on some NPF days (e.g., March 27th and April 1st) are obviously underestimated. It may suggest that the model would not be able to capture effects at a given site during 320 certain periods when the measurements are affected by sub-grid-scale processes (emissions, plumes, etc.). It may be helpful to compare high-resolution simulations with observations in order to address the issue.

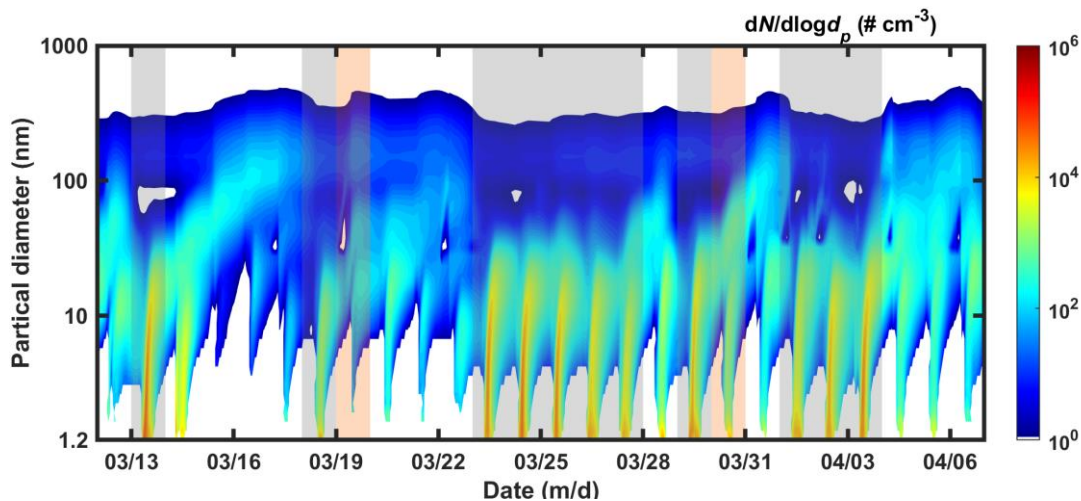


Figure 8. The simulated particle size distributions based on the TIMN scheme. The identified NPF days and undefined days are shadowed by grey and orange background, respectively.

325 The time series of the simulated  $PM_{2.5}$  and  $PM_{10}$  mass concentrations are compared against the measurements during the study period (Figure 9). It is shown that APM generally reproduces the temporal variations of  $PM_{2.5}$  and  $PM_{10}$  mass concentrations, but tends to underestimate high values of  $PM_{2.5}$  and  $PM_{10}$  mass concentrations, possibly due to relatively low spatial resolution and the emission inventory uncertainty. Nevertheless, the correlation coefficients between simulations and observation  $PM_{2.5}$  and  $PM_{10}$  mass concentrations can reach 0.619 and 0.496, respectively, indicating that the simulation  
 330 performance of APM is effective.

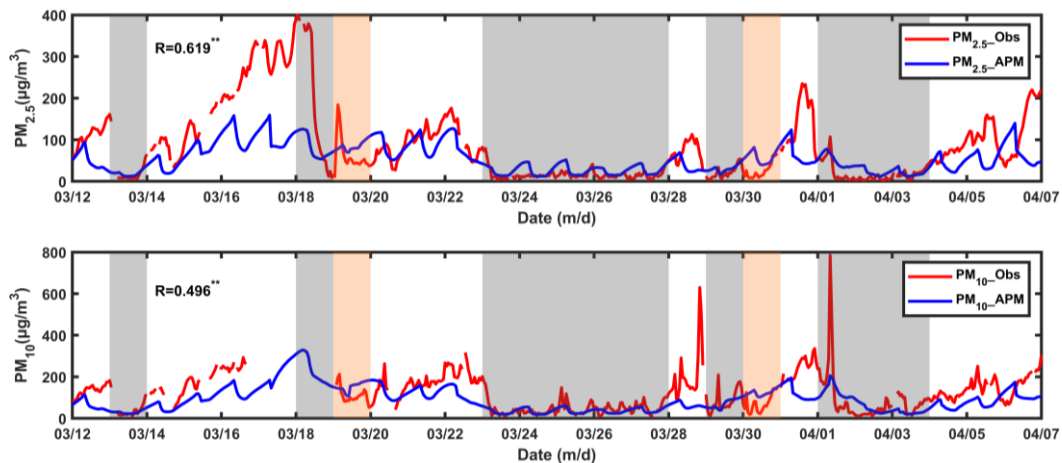


Figure 9. Comparison of observation  $PM_{2.5}$  and  $PM_{10}$  mass concentrations with that in simulation based on APM model during the measurement period. The identified NPF days and undefined days are shadowed by grey and orange background, respectively.

\*\* the correlation coefficient passes the statistical significant test ( $p < 0.01$ ).

335 In summary, in order to evaluate the ability of GEOS-Chem/APM and improve our understanding on nucleation mechanisms, four nucleation schemes are chosen for the model. The BHN scheme and BIMN scheme underestimate the observed particle number concentrations and fail to show significant number concentration fluctuation to distinguish NPF event and non-event event days. The THN scheme well simulates the particle number concentrations on most NPF days except March 18th and April 1st. The TIMN scheme can overall well simulate the total and sub-3 nm particle number concentrations  
340 and nucleation rates in Beijing, which provides a basis for discussing the nucleation mechanism in Beijing. The real nucleation mechanisms in the atmosphere are complex and may involve additional parameters. Besides, further understanding of the nucleation mechanism in Beijing requires more meteorological and precursor gas concentration data in other seasons and model evaluation based on other schemes. The effect of meteorological conditions and precursors on nucleation can be further explored in sensitivity tests focusing on nucleation.

#### 345 **4 Summary and conclusions**

During March 12th to April 6th, 2016 in Beijing, there are 11 typical NPF event days, 13 non-event days and 2 undefined days. The sulfuric acid concentration in Beijing is sufficient to lead to NPF. The meteorological factors have systematical influences on NPF. Our study confirms that low RH is indeed favorable to the occurrence of an NPF event, as found by previous studies. Low RH and  $PM_{2.5}$  mass concentrations reduce CS of condensable gases and coagulation scavenging of new clusters.  
350 In contrast, high  $PM_{2.5}$  concentrations and RH will increase the sinks of vapor responsible for nucleation and growth of clusters.

To understand the applicability of different nucleation schemes in polluted areas such as Beijing and improve our understanding of nucleation mechanisms, the simulations based on GEOS-Chem/APM model are conducted during this observation period. It is found that the simulations with BHN and BIMN schemes systematically underestimate both number concentrations and nucleation rates. TIMN scheme overall has a better performance than the THN scheme in terms of the  
355 simulations of the total and sub-3 nm particle number concentrations and nucleation rates. APM also reproduces the temporal variations of particle matter concentrations, indicating that the simulation performance of APM is effective.  $H_2SO_4$ -amine and

H<sub>2</sub>SO<sub>4</sub>-organics nucleations may also simultaneously contribute to nucleation in polluted urban areas. Some problems should be solved before using the model to address the role of amines in nucleation, which needs further study in the future.

360 It is acknowledged that more observations on NPF are required in order to further understand nucleation mechanisms in Beijing, especially long-term observational data, which is very important to examine the favorable conditions for nucleation events. More detailed and comprehensive comparisons between model predictions and relevant data obtained in various field measurements will help to further improve the understanding of nucleation mechanisms, explain observed nucleation events, and accurately predict air quality.

**Data availability.** Data used in this work have been listed in Sect. 2.1 and acknowledgements.

365 **Author contributions.** KW and XM developed the project idea. KW, XM, and RT designed and conducted the model experiments. KW and XM analyzed the result and wrote the paper. XM and FY proposed scientific suggestions and revised the paper. All coauthors have read and commented on the manuscript.

**Competing interests.** The authors declare that they have no conflict of interest.

370 **Acknowledgements.** This study is supported by the National Key R&D Program of China grants (2019YFA0606802), the National Natural Science Foundation of China grants (42061134009 & 41975002). We are thankful to Prof. Jiang Jingkun for kindly providing new particle formation measurements. We are also grateful to GEOS-Chem Support Team for their management and maintenance of GEOS-Chem model.

## Reference

- Aalto, P., Hämeri, K., Becker, E., Weber, R., Salm, J., Mäkelä, J., Hoell, C., O’ Dowd, C., Hansson, H., Väkevä, M., Koponen, I., Buzorius, G., and Kulmala, M.: Physical characterization of aerosol particles during nucleation events, *Tellus Ser. B: Chem. Phys. Meteor.*, 53, 344-358, <https://doi.org/10.3402/tellusb.v53i4.17127>, 2001.
- 375 An, J., Wang, H., Shen, L., Zhu, B., Zou, J., Gao, J., and Kang, H.: Characteristics of new particle formation events in Nanjing, China: Effect of water-soluble ions, *Atmos. Environ.*, 108, 32-40, <https://doi.org/10.1016/j.atmosenv.2015.01.038>, 2015.

- 380 Cai, R., Yang, D., Fu, Y., Wang, X., Li, X., Ma, Y., Hao, J., Zheng, J., and Jiang, J.: Aerosol surface area concentration: a governing factor in new particle formation in Beijing, *Atmos. Chem. Phys.*, 17, 12327-12340, <https://doi.org/10.5194/acp-17-12327-2017>, 2017a.
- Cai, R., Chen, D.-R., Hao, J., and Jiang, J.: A Miniature Cylindrical Differential Mobility Analyzer for sub-3 nm Particle Sizing, *J. Aerosol. Sci.*, 106, 111–119, <https://doi.org/10.1016/j.jaerosci.2017.01.004>, 2017b.
- 385 Cai, R., Yan, C., Yang, D., Yin, R., Lu, Y., Deng, C., Fu, Y., Ruan, J., Li, X., Kontkanen, J., Zhang, Q., Kangasluoma, J., Ma, Y., Hao, J., Worsnop, D. R., Bianchi, F., Paasonen, P., Kerminen, V.-M., Liu, Y., Wang, L., Zheng, J., Kulmala, M., and Jiang, J.: Sulfuric acid–amine nucleation in urban Beijing, *Atmos. Chem. Phys.*, 21, 2457–2468, <https://doi.org/10.5194/acp-21-2457-2021>, 2021.
- Cai, R., Yin, R., Yan, C., Yang, D., Deng, C., Dada, L., Kangasluoma, J., Kontkanen, J., Halonen, R., Ma, Y., Zhang, X., Paasonen, P., Petäjä, T., Kerminen, V.-M., Liu, Y., Bianchi, F., Zheng, J., Wang, L., Hao, J., Smith, J. N., Donahue, N. M., 390 Kulmala, M., Worsnop, D. R., and Jiang, J.: The missing base molecules in atmospheric acid–base nucleation, *National Science Review*, 9(10), <https://doi.org/10.1093/nsr/nwac137>, 2022.
- Chen, X., Yang, W., Wang, Z., Li, J., Hu, M., An, J., Wu, Q., Wang, Z., Chen, H., Wei, Y., Du, H., and Wang, D.: Improving new particle formation simulation by coupling a volatility-basis set (VBS) organic aerosol module in NAQPMS+APM, *Atmos. Environ.*, 204, 1-11, <https://doi.org/10.1016/j.atmosenv.2019.01.053>, 2019.
- 395 Chu, B., Kerminen, V., Bianchi, F., Yan, C., Petäjä, T., and Kulmala, M.: Atmospheric new particle formation in China, *Atmos. Chem. Phys.*, 19(1), 115-138, <https://doi.org/10.5194/acp-19-115-2019>, 2019.
- Dai, L., Wang, H., Zhou, L., An, J., Tang, L., Lu, C., Yan, W., Liu, R., Kong, S., Chen, M., Lee, S. and Yu, H.: Regional and local new particle formation events observed in the Yangtze River Delta region, China, *J. Geophys. Res.*, 122(4), 2389-2402, <https://doi.org/10.1002/2016JD026030>, 2017.
- 400 Dal Maso, M., Kulmala, M., Riipinen, I., and Wagner, R.: Formation and growth of fresh atmospheric aerosols: Eight years of aerosol size distribution data from SMEAR II, Hyytiälä, Finland, *Boreal Environment Research*, 10, 323–336, 2005.
- Deng, C., Fu, Y., Dada, L., Yan, C., Cai, R., Yang, D., Zhou, Y., Yin, R., Lu, Y., Li, X., Qiao, X., Fan, X., Nie, W., Kontkanen, J., Kangasluoma, J., Chu, B., Ding, A., Kerminen, V., Paasonen, P., Worsnop, R. D., Bianchi, F., Liu, Y., Zheng, J., Wang,

- L., Kulmala, M., and Jiang, J.: Seasonal characteristics of new particle formation and growth in urban Beijing, *Environ. Sci. Technol.*, 54, 8547–8557, <https://doi.org/10.1021/acs.est.0c00808>, 2020.
- 405 Foreback, B., Dada, L., Daellenbach, K. R., Yan, C., Wang, L., Chu, B., Zhou, Y., Kokkonen, T. V., Kurppa, M., Pileci, R. E., Wang, Y., Chan, T., Kangasluoma, J., Zhuohui, L., Guo, Y., Li, C., Baalbaki, R., Kujansuu, J., Fan, X., Feng, Z., Rantala, P., Gani, S., Bianchi, F., Kerminen, V.-M., Petäjä, T., Kulmala, M., Liu, Y., and Paasonen, P.: Measurement report: A multi-year study on the impacts of Chinese New Year celebrations on air quality in Beijing, China, *Atmos. Chem. Phys.*, 22, 11089–11104, <https://doi.org/10.5194/acp-22-11089-2022>, 2022.
- 410 Gong, Y., Hu, M., Cheng, Y., Su, H., Yue, D., Liu, F., Wiedensohler, A., Wang, Z., Kalesse, H., and Liu, S.: Competition of coagulation sink and source rate: New particle formation in the Pearl River Delta of China, *Atmos. Environ.*, 44, 3278–3285, <https://doi.org/10.1016/j.atmosenv.2010.05.049>, 2010.
- Guo, S., Hu, M., Zamora, M., Peng, J., Shang, D., Zheng, J., Du, Z., Wu, Z., Shao, M., Zeng, L., Molina, M., and Zhang, R.: Elucidating severe urban haze formation in China, *Proc Natl Acad Sci USA*, 111, 17373–17378, <https://doi.org/10.1073/pnas.1419604111>, 2014.
- 415 Hamed, A., Korhonen, H., Sihto, S., Joutsensaari, J., Järvinen, H., Petäjä, T., Arnold, F., Nieminen, T., Kulmala, M., Smith, J., Lehtinen, K., and Laaksonen, A.: The role of relative humidity in continental new particle formation, *J. Geophys. Res.*, 116, D03202 <https://doi.org/10.1029/2010jd014186>, 2011.
- 420 Herrmann, E., Ding, A., Kerminen, V., Petäjä, T., Yang, X., Sun, J., Qi, X., Manninen, H., Hakala, J., Nieminen, T., Aalto, P., Kulmala, M., and Fu, C.: Aerosols and nucleation in eastern China: first insights from the new SORPES-NJU station, *Atmos. Chem. Phys.*, 14, 2169–2183, <https://doi.org/10.5194/acp-14-2169-2014>, 2014.
- Hussein, T.: Indoor and outdoor aerosol particle size characterization in Helsinki, *Rep. Ser. Aerosol Sci.*, 74, 1–53, 2005.
- Hu, Y., Zang, Z., Chen, D., Ma, X., Liang, Y., You, W., Pan, X., Wang, L., Wang, D., and Zhang, Z.: Optimization and Evaluation of SO<sub>2</sub> Emissions Based on WRF-Chem and 3DVAR Data Assimilation, *Remote Sens.*, 14, 220, <https://doi.org/10.3390/rs14010220>, 2022
- 425 Jayaratne, R., Pushpawela, B., He, C., Li, H., Gao, J., Chai, F., and Morawska, L.: Observations of particles at their formation sizes in Beijing, China, *Atmos. Chem. Phys.*, 17, 8825–8835, <https://doi.org/10.5194/acp-17-8825-2017>, 2017.

- Kaiser, J.: How dirty air hurts the heart, *Science*, 307, 1858-1859, <https://doi.org/10.1126/science.307.5717.1858b>, 2005.
- 430 Korhonen, P., Kulmala, M., Laaksonen, A., Viisanen, Y., McGraw, R., and Seinfeld, J.: Ternary nucleation of H<sub>2</sub>SO<sub>4</sub>, NH<sub>3</sub>, and H<sub>2</sub>O in the atmosphere, *J. Geophys. Res.*, 104, 26349-26353, <https://doi.org/10.1029/1999jd900784>, 1999.
- Kulmala, M., Laaksonen, A., and Pirjola, L.: Parameterizations for sulfuric acid/water nucleation rates, *J. Geophys. Res.*, 103, 8301-8307, <https://doi.org/10.1029/97jd03718>, 1998.
- Kulmala, M., Kontkanen, J., Junninen, H., Lehtipalo, K., Manninen, H. E., Nieminen, T., Petaja, T., Sipila, M., Schobesberger, S., Rantala, P., Franchin, A., Jokinen, T., Jarvinen, E., Aijala, M., Kangasluoma, J., Hakala, J., Aalto, P. P., Paasonen, P., Mikkila, J., Vanhanen, J., Aalto, J., Hakola, H., Makkonen, U., Ruuskanen, T., Mauldin, R. L., III, Duplissy, J., Vehkamäki, H., Back, J., Kortelainen, A., Riipinen, I., Kurten, T., Johnston, M. V., Smith, J. N., Ehn, M., Mentel, T. F., Lehtinen, K. E. J., Laaksonen, A., Kerminen, V.-M., and Worsnop, D. R.: Direct observations of atmospheric aerosol nucleation, *Science*, 339, 943-946, <https://doi.org/10.1126/science.1227385>, 2013.
- 435 S., Rantala, P., Franchin, A., Jokinen, T., Jarvinen, E., Aijala, M., Kangasluoma, J., Hakala, J., Aalto, P. P., Paasonen, P., Mikkila, J., Vanhanen, J., Aalto, J., Hakola, H., Makkonen, U., Ruuskanen, T., Mauldin, R. L., III, Duplissy, J., Vehkamäki, H., Back, J., Kortelainen, A., Riipinen, I., Kurten, T., Johnston, M. V., Smith, J. N., Ehn, M., Mentel, T. F., Lehtinen, K. E. J., Laaksonen, A., Kerminen, V.-M., and Worsnop, D. R.: Direct observations of atmospheric aerosol nucleation, *Science*, 339, 943-946, <https://doi.org/10.1126/science.1227385>, 2013.
- 440 Kulmala, M., Petaja, T., Kerminen, V. M., Kujansuu, J., Ruuskanen, T., Ding, A. J., Nie, W., Hu, M., Wang, Z. B., Wu, Z. J., Wang, L., and Worsnop, D. R.: On secondary new particle formation in China, *Front. Environ. Sci. Eng.*, 10, 08, <https://doi.org/10.1007/s11783-016-0850-1>, 2016.
- Kulmala, M., Cai, R., Stolzenburg, D., Zhou, Y., Dada, L., Guo, Y., Yan, C., Petäjä, T., Jiang, J., and Kerminen, V.-M.: The contribution of new particle formation and subsequent growth to haze formation, *Environ. Sci.-Atmos.*, 2, 352–361, <https://doi.org/10.1039/D1EA00096A>, 2022.
- 445 <https://doi.org/10.1039/D1EA00096A>, 2022.
- Liu, J., Jiang, J., Zhang, Q., Deng, J., and Hao, J.: A spectrometer for measuring particle size distributions in the range of 3 nm to 10 μm, *Front. Environ. Sci. En.*, 10, 63–72, <https://doi.org/10.1007/s11783-014-0754-x>, 2016.
- Luo, G. and Yu, F.: Simulation of particle formation and number concentration over the Eastern United States with the WRF-Chem + APM model, *Atmos. Chem. Phys.*, 11, 11521-11533, <https://doi.org/10.5194/acp-11-11521-2011>, 2011.
- 450 Merikanto, J., Spracklen, D., Mann, G., Pickering, S., and Carslaw, K.: Impact of nucleation on global CCN, *Atmos. Chem. Phys.*, 9, 8601-8616, <https://doi.org/10.5194/acp-9-8601-2009>, 2009.
- Metzger, A., Verheggen, B., Dommen, J., Duplissy, J., Prevot, A. S., Weingartner, E., Riipinen, I., Kulmala, M., Spracklen, D. V., Carslaw, K. S., and Baltensperger, U.: Evidence for the role of organics in aerosol particle formation under

- atmospheric conditions, *Proceedings of the National Academy of Sciences*, 107(15), 6646–6651,  
455 <https://doi.org/10.1073/pnas.0911330107>, 2010.
- Nieminen, T., Manninen, H. E., Sihto, S. L., Yli-Juuti, T., Mauldin, I. R. L., Petaja, T., Riipinen, I., Kerminen, V. M., and  
Kulmala, M.: Connection of sulfuric acid to atmospheric nucleation in boreal forest, *Environ. Sci. Technol.*, 43(13), 4715-  
4721, <https://doi.org/10.1021/es803152j>, 2009.
- Park, R.: Natural and transboundary pollution influences on sulfate-nitrate-ammonium aerosols in the United States:  
460 Implications for policy, *J. Geophys. Res.*, 109, D15204, <https://doi.org/10.1029/2003jd004473>, 2004.
- Qiao, X., Yan, C., Li, X., Guo, Y., Yin, R., Deng, C., Li, C., Nie, W., Wang, M., Cai, R., Huang, D., Wang, Z., Yao, L., Worsnop,  
D., Bianchi, F., Liu, Y., Donahue, N., Kulmala, M., and Jiang, J.: Contribution of Atmospheric Oxygenated Organic  
Compounds to Particle Growth in an Urban Environment, *Environmental Science & Technology*,  
10.1021/acs.est.1c02095, 2021.
- 465 Qi, X., Ding, A., Nie, W., Petäjä, T., Kerminen, V., Herrmann, E., Xie, Y., Zheng, L., Manninen, H., Aalto, P., Sun, J., Xu, Z.,  
Chi, X., Huang, X., Boy, M., Virkkula, A., Yang, X., Fu, C., and Kulmala, M.: Aerosol size distribution and new particle  
formation in the western Yangtze River Delta of China: 2 years of measurements at the SORPES station, *Atmos. Chem.  
Phys.*, 15, 12445-12464, <https://doi.org/10.5194/acp-15-12445-2015>, 2015.
- Shen, X., Sun, J., Yu, F., Wang, Y., Zhong, J., Zhang, Y., Hu, X., Xia, C., Zhang, S., and Zhang, X.: Enhancement of nanoparticle  
470 formation and growth during the COVID-19 lockdown period in urban Beijing, *Atmos. Chem. Phys.*, 21, 7039–7052,  
<https://doi.org/10.5194/acp-21-7039-2021>, 2021.
- Sipilä, M., Berndt, T., Petäjä, T., Brus, D., Vanhanen, J., Stratmann, F., Patokoski, J., Mauldin, R., Hyvärinen, A., Lihavainen,  
H., and Kulmala, M.: The role of sulfuric acid in atmospheric nucleation, *Science*, 327, 1243-1246,  
<https://doi.org/10.1126/science.1180315>, 2010.
- 475 Sipilä, M., Sarnela, N., Jokinen, T., Henschel, H., Junninen, H., Kontkanen, J., Richters, S., Kangasluoma, J., Franchin, A.,  
Peräkylä, O., Rissanen, M. P., Ehn, M., Vehkamäki, H., Kurten, T., Berndt, T., Petäjä, T., Worsnop, D., Ceburnis, D.,  
Kerminen, V. M., Kulmala, M., and O’Dowd, C.: Molecular-scale evidence of aerosol particle formation via sequential  
addition of HIO<sub>3</sub>, *Nature*, 537, 532–534, <https://doi.org/10.1038/nature19314>, 2016.



- Stockwell, W. and Calvert, J.: The mechanism of the HO-SO<sub>2</sub> reaction, *Atmos. Environ.* (1967), 17, 2231-2235,  
480 [https://doi.org/10.1016/0004-6981\(83\)90220-2](https://doi.org/10.1016/0004-6981(83)90220-2), 1983.
- Sun, Y., Zhu, Y., Meng, H., Liu, B., Liu, Y., Dong, C., Yao, X., Wang, W., and Xue, L.: New particle formation events in  
summer and winter in the coastal atmosphere in Qingdao, China, *Environmental Science*, 42(5), 2133-2142,  
<https://doi.org/10.13227/j.hjlx.202007230>, 2021.
- Tang, L., Shang, D., Fang, X., Wu, Z., Qiu, Y., Chen, S., Li, X., Zeng, L., Guo, S., and Hu, M.: More significant impacts  
485 from new particle formation on haze formation during COVID-19 lockdown, *Geophys. Res. Lett.*, 48, e2020GL091591,  
<https://doi.org/10.1029/2020gl091591>, 2021.
- Tröstl, J., Chuang, W. K., Gordon, H., Heinritzi, M., Yan, C., Molteni, U., Ahlm, L., Frege, C., Bianchi, F., Wagner, R., Simon,  
M., Lehtipalo, K., Williamson, C., Craven, J. S., Duplissy, J., Adamov, A., Almeida, J., Bernhammer, A.-K.,  
Breitenlechner, M., Brilke, S., Dias, A., Ehrhart, S., Flagan, R. C., Franchin, A., Fuchs, C., Guida, R., Gysel, M., Hansel,  
490 A., Hoyle, C. R., Jokinen, T., Junninen, H., Kangasluoma, J., Keskinen, H., Kim, J., Krapf, M., Kuerten, A., Laaksonen,  
A., Lawler, M., Leiminger, M., Mathot, S., Moehler, O., Nieminen, T., Onnela, A., Petaja, T., Piel, F. M., Miettinen, P.,  
Rissanen, M. P., Rondo, L., Sarnela, N., Schobesberger, S., Sengupta, K., Sipila, M., Smith, J. N., Steiner, G., Tome, A.,  
Virtanen, A., Wagner, A. C., Weingartner, E., Wimmer, D., Winkler, P. M., Ye, P., Carslaw, K. S., Curtius, J., Dommen, J.,  
Kirkby, J., Kulmala, M., Riipinen, I., Worsnop, D. R., Donahue, N. M., and Baltensperger, U.: The role of low-volatility  
495 organic compounds in initial particle growth in the atmosphere, *Nature*, 533, 527–531,  
<https://doi.org/10.1038/nature18271>, 2016.
- Wang, Z., Hu, M., Pei, X., Zhang, R., Paasonen, P., Zheng, J., Yue, D., Wu, Z., Boy, M., and Wiedensohler, A.: Connection of  
organics to atmospheric new particle formation and growth at an urban site of Beijing, *Atmos. Environ.*, 103, 7-17,  
<https://doi.org/10.1016/j.atmosenv.2014.11.069>, 2015.
- 500 Weber, R. J., McMurry, P. H., Mauldin, R. L., Tanner, D. J., Eisele, F. L., Clarke, A. D., and Kapustin, V. N.: New particle  
formation in the remote troposphere: a comparison of observations at various sites, *Geophys. Res. Lett.*, 26(3), 307-310,  
<https://doi.org/10.1029/1998gl900308>, 1999.

- 505 Wu, H., Li, Z., Li, H., Luo, K., Wang, Y., Yan, P., Hu, F., Zhang, F., Sun, Y., Shang, D., Liang, C., Zhang, D., Wei, J., Wu, T., Jin, X., Fan, X., Cribb, M., Fischer, M., Kulmala, M., and Petäjä, T.: The impact of the atmospheric turbulence-development tendency on new particle formation: a common finding on three continents, *National Science Review*, 8(3), 140-150, <https://doi.org/10.1093/nsr/nwaa157>, 2020.
- Wu, Z., Hu, M., Liu, S., Wehner, B., Bauer, S., Maßling, A., Wiedensohler, A., Petäjä, T., Dal Maso, M., and Kulmala, M.: New particle formation in Beijing, China: Statistical analysis of a 1-year data set, *J. Geophys. Res.*, 112, D09209, <https://doi.org/10.1029/2006jd007406>, 2007.
- 510 Wu, Z., Hu, M., Lin, P., Liu, S., Wehner, B., and Wiedensohler, A.: Particle number size distribution in the urban atmosphere of Beijing, China, *Atmos. Environ.*, 42, 7967-7980, <https://doi.org/10.1016/j.atmosenv.2008.06.022>, 2008.
- Xiao, M., Hoyle, C. R., Dada, L., Stolzenburg, D., Kürten, A., Wang, M., Lamkaddam, H., Garmash, O., Mentler, B., Molteni, U., Baccarini, A., Simon, M., He, X.-C., Lehtipalo, K., Ahonen, L. R., Baalbaki, R., Bauer, P. S., Beck, L., Bell, D., Bianchi, F., Brilke, S., Chen, D., Chiu, R., Dias, A., Duplissy, J., Finkenzeller, H., Gordon, H., Hofbauer, V., Kim, C., Koenig, T. K., Lampilahti, J., Lee, C. P., Li, Z., Mai, H., Makhmutov, V., Manninen, H. E., Marten, R., Mathot, S., Mauldin, R. L., Nie, W., Onnela, A., Partoll, E., Petäjä, T., Pfeifer, J., Pospisilova, V., Quéléver, L. L. J., Rissanen, M., Schobesberger, S., Schuchmann, S., Stozhkov, Y., Tauber, C., Tham, Y. J., Tomé, A., Vazquez-Pufleau, M., Wagner, A. C., Wagner, R., Wang, Y., Weitz, L., Wimmer, D., Wu, Y., Yan, C., Ye, P., Ye, Q., Zha, Q., Zhou, X., Amorim, A., Carslaw, K., Curtius, J., Hansel, A., Volkamer, R., Winkler, P. M., Flagan, R. C., Kulmala, M., Worsnop, D. R., Kirkby, J., Donahue, N. M., Baltensperger, U., El Haddad, I., and Dommen, J.: The driving factors of new particle formation and growth in the polluted boundary layer, *Atmos. Chem. Phys.*, 21, 14275–14291, <https://doi.org/10.5194/acp-21-14275-2021>, 2021.
- 520 Xiao, S., Wang, M., Yao, L., Kulmala, M., Zhou, B., Yang, X., Chen, J., Wang, D., Fu, Q., Worsnop, D., and Wang, L.: Strong atmospheric new particle formation in winter in urban Shanghai, China, *Atmos. Chem. Phys.*, 15, 1769-1781, <https://doi.org/10.5194/acp-15-1769-2015>, 2015.
- Yan, C., Yin, R., Lu, Y., Dada, L., Yang, D., Fu, Y., Kontkanen, J., Deng, C., Garmash, O., Ruan, J., Baalbaki, R., Schervish, M., Cai, R., Bloss, M., Chan, T., Chen, T., Chen, Q., Chen, X., Chen, Y., Chu, B., Dällenbach, K., Foreback, B., He, X., Heikkinen, L., Jokinen, T., Junninen, H., Kangasluoma, J., Kokkonen, T., Kurppa, M., Lehtipalo, K., Li, H., Li, H., Li,

- X., Liu, Y., Ma, Q., Paasonen, P., Rantala, P., Pileci, R. E., Rusanen, A., Sarnela, N., Simonen, P., Wang, S., Wang, W., Wang, Y., Xue, M., Yang, G., Yao, L., Zhou, Y., Kujansuu, J., Petäjä, T., Nie, W., Ma, Y., Ge, M., He, H., Donahue, N. M., Worsnop, D. R., Veli-Matti, K., Wang, L., Liu, Y., Zheng, J., Kulmala, M., Jiang, J., and Bianchi, F.: The Synergistic Role of Sulfuric Acid, Bases, and Oxidized Organics Governing New-Particle Formation in Beijing, *Geophys. Res. Lett.*, 48, e2020GL091944, <https://doi.org/10.1029/2020gl091944>, 2021.
- 530
- Yao, L., Garmash, O., Bianchi, F., Zheng, J., Yan, C., Kontkanen, J., Junninen, H., Mazon, S., Ehn, M., Paasonen, P., Sipilä, M., Wang, M., Wang, X., Xiao, S., Chen, H., Lu, Y., Zhang, B., Wang, D., Fu, Q., Geng, F., Li, L., Wang, H., Qiao, L., Yang, X., Chen, J., Kerminen, V., Petäjä, T., Worsnop, D., Kulmala, M., and Wang, L.: Atmospheric new particle formation from sulfuric acid and amines in a Chinese megacity, *Science*, 361, 278-281, <https://doi.org/10.1126/science.aao4839>, 2018.
- 535
- Yu, F.: Effect of ammonia on new particle formation: A kinetic H<sub>2</sub>SO<sub>4</sub>-H<sub>2</sub>O-NH<sub>3</sub> nucleation model constrained by laboratory measurements, *J. Geophys. Res.*, 111, D01204, <https://doi.org/10.1029/2005JD005968>, 2006a.
- 540
- Yu, F.: From molecular clusters to nanoparticles: second-generation ion-mediated nucleation model, *Atmos. Chem. Phys.*, 6, 5193-5211, <https://doi.org/10.5194/acp-6-5193-2006>, 2006b.
- Yu, F.: Improved quasi-unary nucleation model for binary H<sub>2</sub>SO<sub>4</sub>-H<sub>2</sub>O homogeneous nucleation, *J. Chem. Phys.*, 127, 054301, <https://doi.org/10.1063/1.2752171>, 2007.
- Yu, F.: Updated H<sub>2</sub>SO<sub>4</sub>-H<sub>2</sub>O binary homogeneous nucleation look-up tables, *J. Geophys. Res.*, 113, D24201, <https://doi.org/10.1029/2008jd010527>, 2008.
- 545
- Yu, F.: A secondary organic aerosol formation model considering successive oxidation aging and kinetic condensation of organic compounds: global scale implications, *Atmos. Chem. Phys.*, 11, 1083–1099, <https://doi.org/10.5194/acp-11-1083-2011>, 2011.
- Yu, F. and Luo, G.: Simulation of particle size distribution with a global aerosol model: contribution of nucleation to aerosol and CCN number concentrations, *Atmos. Chem. Phys.*, 9, 7691-7710, <https://doi.org/10.5194/acp-9-7691-2009>, 2009.
- 550

- Yu, F. and Luo, G.: Oceanic dimethyl sulfide emission and new particle formation around the coast of Antarctica: a modeling study of seasonal variations and comparison with measurements, *Atmosphere*, 1(1), 34-50, <https://doi.org/10.3390/atmos1010034>, 2010.
- 555 Yu, F. and Turco, R.: Ultrafine aerosol formation via ion-mediated nucleation, *Geophys. Res. Lett.*, 27(6), 883-886, <https://doi.org/10.1029/1999gl011151>, 2000.
- Yu, F. and Turco, R. P.: The size-dependent charge fraction of sub-3-nm particles as a key diagnostic of competitive nucleation mechanisms under atmospheric conditions, *Atmos. Chem. Phys.*, 11, 9451–9463, <https://doi.org/10.5194/acp-11-9451-2011>, 2011.
- 560 Yu, F., Wang, Z., Luo, G., and Turco, R. Ion-mediated nucleation as an important global source of tropospheric aerosols, *Atmos. Chem. Phys.*, 8, 2537-2554, <https://doi.org/10.5194/acp-8-2537-2008>, 2008.
- Yu, F., Luo, G., Bates, T., Anderson, B., Clarke, A., Kapustin, V., Yantosca, R., Wang, Y., and Wu, S.: Spatial distributions of particle number concentrations in the global troposphere: simulations, observations, and implications for nucleation mechanisms, *J. Geophys. Res.*, 115, D17205, <https://doi.org/10.1029/2009jd013473>, 2010.
- 565 Yu, F., Nadykto, A. B., Herb, J., Luo, G., Nazarenko, K. M., and Uvarova, L. A.: H<sub>2</sub>SO<sub>4</sub>–H<sub>2</sub>O–NH<sub>3</sub> ternary ion-mediated nucleation (TIMN): kinetic-based model and comparison with CLOUD measurements, *Atmos. Chem. Phys.*, 18, 17451–17474, <https://doi.org/10.5194/acp-18-17451-2018>, 2018.
- Yu, F., Nadykto, A. B., Luo, G., and Herb, J.: H<sub>2</sub>SO<sub>4</sub>–H<sub>2</sub>O binary and H<sub>2</sub>SO<sub>4</sub>–H<sub>2</sub>O–NH<sub>3</sub> ternary homogeneous and ion-mediated nucleation: lookup tables version 1.0 for 3-D modeling application, *Geosci. Model Dev.*, 13, 2663–2670, <https://doi.org/10.5194/gmd-13-2663-2020>, 2020.
- 570 Zhang, R., Khalizov, A., Wang, L., Hu, M., and Xu, W.: Nucleation and growth of nanoparticles in the atmosphere, *Chem. Rev.*, 112(3), 1957-2011, <https://doi.org/10.1021/cr2001756>, 2012.
- Zheng, J., Hu, M., Zhang, R., Yue, D., Wang, Z., Guo, S., Li, X., Bohn, B., Shao, M., He, L., Huang, X., Wiedensohler, A., and Zhu, T.: Measurements of gaseous H<sub>2</sub>SO<sub>4</sub> by AP-ID-CIMS during CARE Beijing 2008 Campaign, *Atmos. Chem. Phys.*, 11, 7755–7765, <https://doi.org/10.5194/acp-11-7755-2011>, 2011.

- 575 Zheng, J., Yang, D., Ma, Y., Chen, M., Cheng, J., Li, S., and Wang, M.: Development of a new corona discharge based ion source for high resolution time-of-flight chemical ionization mass spectrometer to measure gaseous H<sub>2</sub>SO<sub>4</sub> and aerosol sulfate, *Atmos. Environ.*, 119, 167–173, <https://doi.org/10.1016/j.atmosenv.2015.08.028>, 2015.
- Zhou, Y., Dada, L., Liu, Y., Fu, Y., Kangasluoma, J., Chan, T., Yan, C., Chu, B., Daellenbach, K., Bianchi, F., Kokkonen, T., Liu, Y., Kujansuu, J., Kerminen, V., Petäjä, T., Wang, L., Jiang, J., and Kulmala, M.: Variation of size-segregated particle number concentrations in wintertime Beijing, *Atmos. Chem. Phys.*, 20, 1201-1216, <https://doi.org/10.5194/acp-20-1201-2020>, 2020.
- 580